Heterodimeric coiled-coil interactions of human $GABA_B$ receptor

Svetlana Burmakina[a,1], Yong Geng[a,1], Yan Chen[a], and Qing R. Fan[a,b,2]

Departments of [a]Pharmacology and [b]Pathology and Cell Biology, Columbia University, New York, NY 10032

Edited* by Wayne A. Hendrickson, Columbia University, New York, NY, and approved April 4, 2014 (received for review January 6, 2014)

Metabotropic $GABA_B$ receptor is a G protein-coupled receptor that mediates inhibitory neurotransmission in the CNS. It functions as an obligatory heterodimer of $GABA_B$ receptor 1 (GBR1) and $GABA_B$ receptor 2 (GBR2) subunits. The association between GBR1 and GBR2 masks an endoplasmic reticulum (ER) retention signal in the cytoplasmic region of GBR1 and facilitates cell surface expression of both subunits. Here, we present, to our knowledge, the first crystal structure of an intracellular coiled-coil heterodimer of human $GABA_B$ receptor. We found that polar interactions buried within the hydrophobic core determine the specificity of heterodimer pairing. Disruption of the hydrophobic coiled-coil interface with single mutations in either subunit impairs surface expression of GBR1, confirming that the coiled-coil interaction is required to inactivate the adjacent ER retention signal of GBR1. The coiled-coil assembly buries an internalization motif of GBR1 at the heterodimer interface. The ER retention signal of GBR1 is not part of the core coiled-coil structure, suggesting that it is sterically shielded by GBR2 upon heterodimer formation.

The major inhibitory neurotransmitter in the CNS is GABA. Metabotropic $GABA_B$ receptor is a G protein-coupled receptor (GPCR) that mediates slow synaptic inhibition (1, 2). It constitutes an important drug target for many neurological disorders, including epilepsy, spasticity, anxiety, and nociception (1, 2).

Formation of a functional $GABA_B$ receptor requires the heterodimeric assembly of $GABA_B$ receptor 1 (GBR1) and $GABA_B$ receptor 2 (GBR2) subunits (3–7). Both consist of an N-terminal extracellular domain, a seven-helix transmembrane domain, and a C-terminal intracellular domain. The intracellular domain of each subunit contains a stretch of coiled-coil sequence, and interaction between the coiled-coil helices is partly responsible for $GABA_B$ receptor heterodimerization (5, 8).

The intracellular region of $GABA_B$ receptor hosts elements that control receptor trafficking (9). Specifically, GBR1 has a di-leucine internalization signal (EKSRLL) (9) and an endoplasmic reticulum (ER) retention signal (RSRR) (9–11) located within or near its coiled-coil domain (9). GBR1 is trapped within the ER when expressed alone (12) but can reach the cell surface upon association with GBR2 (9, 11). Mutation or removal of the ER retention signal in GBR1 results in plasma membrane expression of GBR1 (9–11). Furthermore, interaction between the coiled-coil domains of GBR1 and GBR2 masks this ER retention signal to facilitate the cell surface expression of both subunits (9–11). Although mutation of the di-leucine motif itself is not sufficient to release GBR1 from intracellular retention, it enhances cell surface expression of various GBR1 mutants that lack the ER retention signal (9).

The coiled-coil domain of GBR1 associates with a number of intracellular proteins involved in trafficking, including the coat protein complex I (COPI) (13), the scaffolding protein 14-3-3 (13, 14), the GPCR interacting scaffolding protein GISP (15), and the guanidine exchange factor msec7-1 (16). In particular, COPI specifically recognizes the ER retention signal sequence of GBR1 and is involved in the intracellular retention of GBR1 (13). The msec7-1 protein increases the cell surface expression of $GABA_B$ receptor by binding to the di-leucine internalization motif (16).

Despite its important role in $GABA_B$ receptor assembly and trafficking, the atomic details of the coiled-coil interaction between subunits are not known. In this study, we present the crystal structure of a GBR1/GBR2 coiled-coil heterodimer and identify specific contacts at the heterodimer interface that control the surface expression of GBR1.

Results

Heterodimerization of GBR1 and GBR2 Coiled-Coils. The intracellular coiled-coil domains of both human GBR1b (GBR1bcc) and GBR2 (GBR2cc) were separately expressed in bacteria. The cytoplasmic region is identical for the most abundant GBR1 isoforms, GBR1a and GBR1b (17). To determine the boundary of the coiled-coil domain within each subunit, we carried out coiled-coil predictions using the programs COILS (18) and Paircoil2 (19). Based on these predictions, we generated several pairs of GBR1b and GBR2 constructs with different N- and C-terminal truncations of their intracellular regions. One pair of constructs (GBR1bcc1 and GBR2cc1) consists of the core coiled-coil sequences of GBR1b and GBR2, which have a high probability of adopting a coiled-coil conformation ($P \geq 0.8$, calculated using COILS algorithm) (Fig. S1). Another longer pair of constructs (GBR1bcc2 and GBR2cc2) also includes an eight-residue C-terminal extension for each subunit, which has a low probability of forming a coiled-coil ($P \leq 0.25$). This extension in GBR1bcc2 contains the ER retention signal sequence RSRR of GBR1, and GBR2cc2 contains the corresponding sequence in GBR2. All of these constructs were expressed as soluble proteins in the bacterial cytosol.

Heterodimerization of the coiled-coil regions of GBR1b and GBR2 can be demonstrated by native gel shift assay (Fig. 1 *A* and *B*). The appearance of a novel band, along with the disappearance of the individual subunits, was observed for the mixture of

Significance

Human $GABA_B$ receptor transmits inhibitory signals in the brain. Defects in the receptor are linked to several neurological diseases, including epilepsy and spasticity. The $GABA_B$ receptor consists of two subunits, $GABA_B$ receptor 1 (GBR1) and $GABA_B$ receptor 2 (GBR2). GBR1 is trapped inside the cell because it contains an endoplasmic reticulum retention signal that targets the receptor to the intracellular compartment. This retention signal is masked by coiled-coil interaction between GBR1 and GBR2 when the two subunits associate. The crystal structure of a coiled-coil complex between the $GABA_B$ receptor subunits reveals the heterodimeric interaction that is responsible for facilitating the surface transport of the intact receptor.

Author contributions: Q.R.F. designed research; S.B., Y.G., Y.C., and Q.R.F. performed research; S.B., Y.G., and Q.R.F. analyzed data; and Q.R.F. wrote the paper.

The authors declare no conflict of interest.

*This Direct Submission article had a prearranged editor.

Data deposition: The atomic coordinates have been deposited in the Protein Data Bank, www.pdb.org (PDB ID code 4PAS).

[1]S.B. and Y.G. contributed equally to this work.

[2]To whom correspondence should be addressed. E-mail: qf13@columbia.edu.

This article contains supporting information online at www.pnas.org/lookup/suppl/doi:10.1073/pnas.1400081111/-/DCSupplemental.

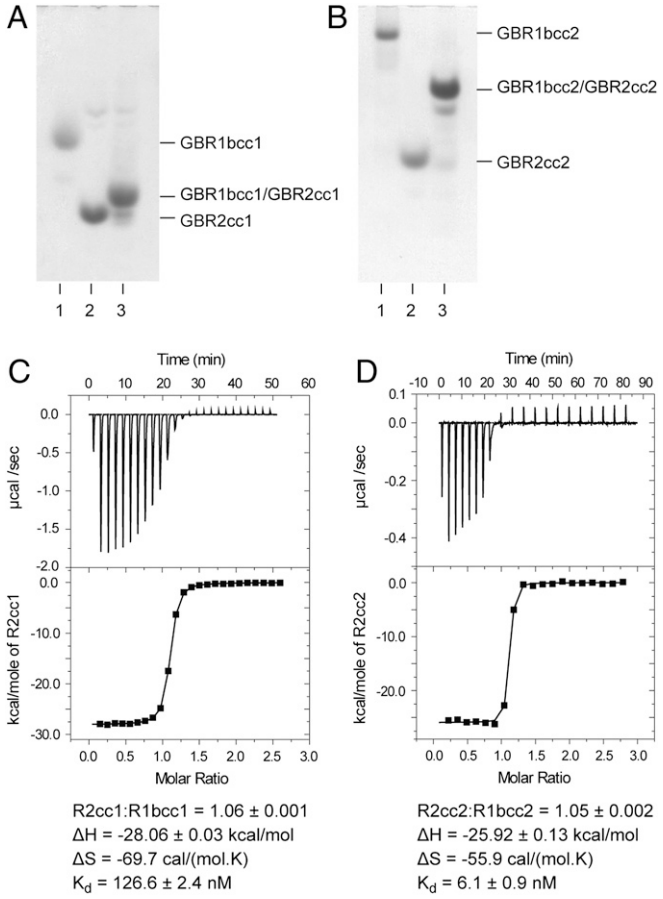

Fig. 1. Heterodimerization of GBR1bcc and GBR2cc. (*A* and *B*) Native gel electrophoresis (8–25%) shows the binding between GBR1bcc and GBR2cc. Lane 1 is GBR1bcc, lane 2 is GBR2cc, and lane 3 contains their mixture. The binding reaction was carried out between GBR1bcc1 and GBR2cc1 (*A*) and between GBR1bcc2 and GBR2cc2 (*B*). (*C* and *D*) Thermodynamics of the interactions between GBR1bcc1 and GBR2cc1 (*C*) and between GBR1bcc2 and GBR2cc2 (*D*) are shown. Each panel presents raw data (*Upper*) and heat data after peak integration and subtraction of control titration (*Lower*). Heat changes are plotted as a function of the molar ratio of GBR2cc to GBR1bcc for each injection. The curve represents the best nonlinear least-squares fitting of the data to a one-site binding model. ΔH, binding enthalpy, K_d, dissociation constant of the interaction; N, binding stoichiometry; ΔS, entropy value.

GBR1bcc1 and GBR2cc1 as well as that of GBR1bcc2 and GBR2cc2, indicating that both pairs interact to form complexes.

To assemble a coiled-coil heterodimer, the individual subunits were expressed and purified separately and then combined to form a complex. Upon gel filtration chromatography, the GBR1bcc1/GBR2cc1 complex has a shorter retention time than the individual subunits because of its larger molecular mass. The purified complex contains both subunits as confirmed by N-terminal sequencing. Similarly, complex formation was observed for GBR1bcc2 and GBR2cc2.

The direct binding between each pair of GBR1b and GBR2 coiled-coils was measured by isothermal titration calorimetry (ITC) (Fig. 1 *C* and *D*). The experimentally determined binding stoichiometry is 1:1 for both pairs of coiled-coils. The interaction between GBR1bcc1 and GBR2cc1 has a dissociation constant of 126.6 ± 2.4 nM, with an enthalpic contribution (ΔH) of −28.03 ± 0.03 kcal·mol^{-1} and an entropic factor (−TΔS) of 19.32 ± 0.02 kcal· mol^{-1}. The affinity between GBR1bcc2 and GBR2cc2 is higher with a dissociation constant of 6.1 ± 0.9 nM, and the corresponding enthalpic contribution and entropic factor are −25.92 ± 0.03 kcal· mol^{-1} (ΔH) and 15.49 ± 0.02 kcal·mol^{-1} (−TΔS), respectively.

The thermodynamics of both reactions resemble those of the protein folding process, and are characterized by favorable enthalpic contributions and unfavorable entropic changes. The binding between the shorter constructs GBR1bcc1 and GBR2cc1 is associated with a much greater entropic penalty (−TΔS), and therefore a higher dissociation constant. On the other hand, the enthalpy change (ΔH) is slightly more favorable for the binding between GBR1bcc1 and GBR2cc1, indicating that the heterodimeric interactions (including hydrogen bonds, ionic salt bridges, and van der Waals contacts) are more extensive between the shorter pair. This observation suggests that the C-terminal flanking regions in the longer constructs GBR1bcc2 and GBR2cc2 do not contribute additional heterodimeric contacts. The thermodynamic measurements are consistent with this region being in a flexible conformation in both subunits.

Structure of a GBR1bcc/GBR2cc Heterodimer. Single crystals were obtained for the heterodimeric complex formed by the pair of coiled-coil constructs GBR1bcc1 and GBR2cc1. These crystals diffracted to a resolution of 1.62 Å. They belong to the space group $C222_1$ (a = 46.3 Å, b = 54.2 Å, c = 54.9 Å), and have one heterodimer per asymmetrical unit. Crystals of SeMet-substituted GBR1bcc1/GBR2cc1 complex were prepared for phasing; these crystals diffracted to a resolution of 1.77 Å. The structure of the GBR1bcc1/GBR2cc1 heterodimer was solved by the multiwavelength anomalous diffraction (MAD) method (20) using a three-wavelength dataset collected from a single SeMet crystal. The structure was refined against the native dataset at 1.62 Å to a final crystallographic R factor of 19.4% (R_{free} = 21.7%) (Tables S1 and S2 and Fig. S2). In the final model, five N-terminal and one C-terminal residues of GBR1bcc1, as well as two C-terminal residues of GBR2cc1, are not visible in the electron density maps, indicating that they are disordered.

The overall structure of the GBR1bcc1/GBR2cc1 complex consists of a left-handed and two-stranded parallel coiled-coil (Fig. 2*A*). The heterodimer forms a twisted stalk that is ∼61 Å long and 22 Å wide. The helices have 3.61 residues per turn and a rise of 1.51 Å per residue. These parameters yield an average pitch of 153.3 Å for the two-stranded coiled-coil and a mean supercoil radius of 4.89 Å. Compared with a classic two-stranded coiled-coil structure, such as the homodimeric transcriptional activator GCN4-p1 leucine zipper (21), the GBR1bcc1/GBR2cc1 heterodimer features a much longer pitch, and therefore a more gradual completion of a full turn of the supercoil (Table S3).

Heterodimer Interface. Both GBR1bcc1 and GBR2cc1 exhibit the characteristic heptad periodicity of coiled-coils (22). The heptad repeats are denoted $(a\text{-}b\text{-}c\text{-}d\text{-}e\text{-}f\text{-}g)_n$ in GBR1bcc1 and $(a'\text{-}b'\text{-}c'\text{-}d'\text{-}e'\text{-}f'\text{-}g')_n$ in GBR2cc1 (Fig. 2 *B* and *C*). The GBR1bcc1/GBR2cc1 complex contains five complete heptad repeats and additional coiled-coil elements at both ends. Formation of the GBR1bcc1/GBR2cc1 heterodimer buries ∼2,006 Å^2 of solvent-accessible surface area.

The packing of the GBR1bcc1/GBR2cc1 heterodimer follows the "knobs-into-holes" pattern proposed by Crick (23), where a residue at an a or d position of one helix (knob) packs into a space surrounded by four side chains of the partner helix (hole). The intercalating side chains form the hydrophobic core of the heterodimeric coiled-coil (Fig. 3 *A* and *B* and Table S4). Residues at the a and d positions of the GBR1bcc1/GBR2cc1 complex structure are mostly hydrophobic. The d residues are predominantly leucines, whereas the a residues consist of a mixture of Leu, Ile, and Val. Studies based on GCN4 leucine zipper suggest that the distinct local geometries at the a and d positions impose different preferences for hydrophobic residues (24). Specifically, the presence of Ile and Val at a positions and Leu at d positions promotes the formation of dimers (22, 24). The amino acid nature at the hydrophobic core of the GBR1bcc1/GBR2cc1 complex largely conforms to this trend.

The heterodimer interface of the GBR1bcc1/GBR2cc1 complex is also stabilized by hydrogen-bonding interactions (Fig. 4

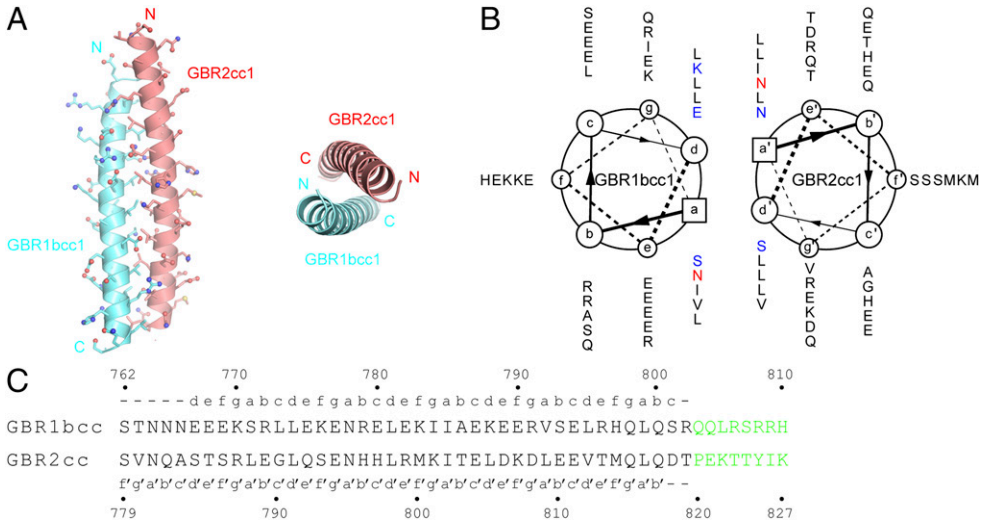

Fig. 2. Structure of the GBR1bcc1/GBR2cc1 heterodimer. (*A*) Ribbon diagram of the GBR1bcc1/GBR2cc1 heterodimer structure shown in two views that are related by 90° about the horizontal axis. GBR1bcc1 and GBR2cc1 are shown in cyan and red, respectively. Side chains are represented by ball and stick models. (*B*) Helical wheel projection of the residues in the heterodimeric GBR1bcc1/GBR2cc1 complex. The structure is viewed from the N termini of GBR1bcc1 and GBR2cc1. The coiled-coil sequence is read from N termini to C termini outward from the wheel. Coiled-coil heptad positions are marked as *a* to *g* for GBR1bcc1 and as *a′* to *g′* for GBR2cc1. The Asn residues that form a buried hydrogen bond at the interface are colored red. Other polar residues at the coiled-coil interface are colored blue. (*C*) Protein sequences of GBR1bcc and GBR2cc constructs. Residues included in the GBR1bcc1 and GBR2cc1 constructs are indicated in black. GBR1bcc2 and GBR2cc2 constructs also contain additional C-terminal flanking residues, which are colored green. Coiled-coil heptad positions are labeled for residues that are visible in the GBR1bcc1/GBR2cc1 crystal structure. Disordered residues are marked with a dash.

A and *B* and Table S4). A prominent feature of the GBR1bcc1/GBR2cc1 structure is a network of hydrogen bonds at its center. This network includes a pair of hydrogen-bonded Asn residues (Asn778 of GBR1b and Asn795′ of GBR2) buried at the heterodimer interface. The Asn residues occupy a pair of corresponding *a* and *a′* positions in GBR1bcc1 and GBR2cc1, respectively. A similar Asn-Asn contact was observed in the crystal structure of GCN4 (21). Analysis of GCN4 leucine zipper and other designed coiled-coils suggests that the presence of polar residues in the generally hydrophobic core introduces specificity for the coiled-coil pairing (25–28). In particular, the presence of Asn residues at *a* positions favors the formation of a parallel, dimeric coiled-coil.

In the structure of the GBR1bcc1/GBR2cc1 complex, the central Asn-Asn contact is surrounded by additional hydrogen bonds that wrap around the coiled-coil in a belt-like fashion (Fig. 4 *A* and *B*). In addition to contacting each other, both Asn residues form intermolecular hydrogen bonds with other neighboring residues from the partner helix. Specifically, Asn778 of GBR1b contacts two other GBR2cc1 residues, Glu794′ at a *g′* position and Leu791 at a *d′* position. Asn795′ of GBR2 makes a hydrogen bond to Glu777 of GBR1b at a *g* position. Furthermore, the hydrogen bond network of the Asn residues is enclosed at both sides by two salt bridges (GBR1b-Glu777/GBR2-Arg799′ and GBR1b-Arg779/GBR2-Glu794′). This hydrogen bond cluster is formed by an asymmetrical pair of sequences from the two subunits: $_{777}$ENR$_{779}$ of GBR1b and $_{794}$ENxxxR$_{799}$ of GBR2.

In addition to the central cluster, there are interfacial hydrogen-bonded contacts at both ends of the coiled-coil structure (Fig. 4 *A* and *B*). The hydrogen bond at the N-terminal end involves Glu767 of GBR1b and Thr785′ of GBR2. The salt bridge close to the C-terminal end is formed by Lys788 of GBR1b and Asp806′ of GBR2. Both contacts involve a GBR1b residue at a *d* position and a GBR2 residue at the neighboring *e′* position. The extensive hydrogen-bonded interactions along the coiled-coil structure enhance the specificity of heterodimeric pairing between GBR1bcc1 and GBR2cc1 because at least some of the hydrogen-bonding requirements cannot be satisfied in a homodimeric setting.

Several residues that are important for regulating the surface expression of GABA$_B$ receptor are found at the heterodimer interface (Fig. 3 *A* and *B*). First, the di-leucine internalization motif of GBR1b ($_{769}$EKSRLL$_{774}$) is located at the coiled-coil interface, with the two Leu residues occupying *c* and *d* positions, respectively. Furthermore, Leu774 of GBR1b is completely buried within the hydrophobic core of the coiled-coil structure. As a result, the coiled-coil interactions between GBR1b and GBR2 directly mask the di-leucine motif of GBR1b. Second, the phosphorylation state of GABA$_B$ receptor affects its cell surface stability (29–31). Specifically, dephosphorylation of Ser784′ in GBR2 is associated with decreased expression of the receptor at the neuronal plasma membrane (31). Ser784′ occupies a *d′* position in GBR2. It caps the N-terminal end of the coiled-coil together with Glu767 of GBR1b, the first ordered residue of GBR1bcc1. As a result, the side chain of Ser784′ is solvent-exposed for phosphorylation and dephosphorylation despite being located at the interface.

Effect of Single Coiled-Coil Mutations on Receptor Trafficking. We introduced point mutations at the heterodimer interface of the GBR1b/GBR2 coiled-coil structure and monitored their effect on the surface trafficking of GBR1b (Fig. 5 and Figs. S3 and S4). Full-length GBR1b and GBR2 were tagged at the N terminus immediately after the signal peptide with Flag and HA epitopes, respectively. Cell surface expression of each subunit was measured by two different methods: (*i*) direct quantification of immunofluorescence on intact cells and (*ii*) biotinylation of surface proteins followed by Western blot analyses. Furthermore, the surface expression was normalized with the total expression level measured after permeabilization of cells. As expected, wild-type GBR2 (GBR2-wt) alone was fully expressed at the cell surface; wild-type GBR1b (GBR1b-wt) alone was retained within the cell, and was only trafficked to the cell surface when it was coexpressed with GBR2-wt.

To test the effect of GBR1b coiled-coil mutations, full-length GBR1b carrying a single mutation at an *a* or *d* position was coexpressed with GBR2-wt. We found that substituting the hydrophobic residues at the coiled-coil interface with charged residues significantly impaired cell surface expression of GBR1b

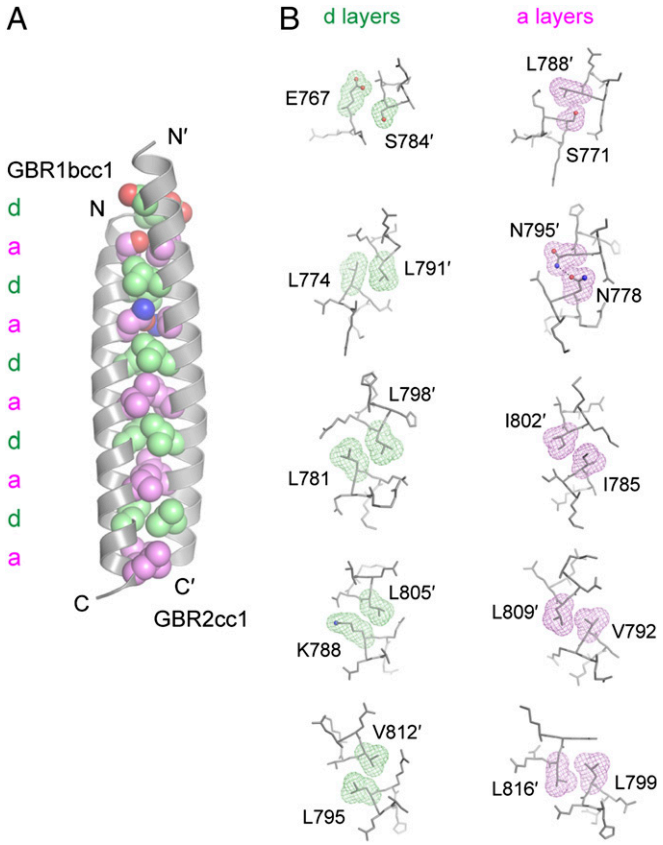

Fig. 3. Hydrophobic layers of the GBR1bcc1/GBR2cc1 core. (*A*) Ribbon diagram of GBR1bcc1/GBR2cc1 heterodimer (gray) shows the side chains of the *a* (magenta) and *d* (green) layers as van der Waals spheres. (*B*) Geometry of individual coiled-coil *a* and *d* layers is shown.

(Fig. 5 *A*–*C* and Fig. S3). These hydrophobic residues include Leu774, Leu781, Ile785, Val792, and Leu795 of GBR1b. In particular, the single mutations L781D and I785D at the center of the coiled-coil were the most disruptive. Similar effects on GBR1b trafficking were observed when the mutations were introduced at the corresponding positions in GBR2, even though none of the mutations affected the surface expression of GBR2 itself (Fig. 5 *D*–*F* and Fig. S4). The positions in GBR2 that are critical for the surface transport of GBR1 include Leu791′, Leu798′, Leu805′, Leu809′, and Val812′, with Leu790′ and Leu805′ being the least tolerant of substitutions. These results confirmed that the coiled-coil interactions between GBR1b and GBR2 are responsible for shielding the ER retention signal of GBR1b. Furthermore, a single mutation of the key interfacial residues was capable of disrupting the masking effect.

Discussion

The intracellular coiled-coil regions of metabotropic $GABA_B$ receptor mediate heterodimer formation of the GBR1 and GBR2 subunits, and control the cell surface expression of GBR1. We found that the core coiled-coil domains of GBR1b and GBR2 directly bind to each other with high affinity. We also assembled a GBR1b/GBR2 coiled-coil heterodimer and determined its crystal structure to high resolution. Specificity of the heterodimer interaction is mediated by intermolecular hydrogen bonds along the coiled-coil.

The GBR1b/GBR2 coiled-coil structure provides insights on the mechanism by which the different trafficking signals located within GBR1 are inactivated. The di-leucine internalization motif of GBR1 directly interacts with GBR2 as part of the coiled-coil structure, and is buried at the heterodimer interface. In contrast, access to the ER retention signal RSRR appears to be blocked by steric hindrance.

Our data suggest that the ER retention signal in GBR1b is not part of the core coiled-coil structure. First, predictions by the COILS and Paircoil2 programs indicate that it has a low probability of adopting a coiled-coil conformation ($P \approx 0.1$ based on the COILS algorithm). Rather, it is located immediately adjacent to the core coiled-coil sequence ($P \geq 0.8$). Second, our thermodynamic measurements suggest that the region containing the ER retention signal and its counterpart in GBR2 do not contribute to heterodimer formation. Using ITC, we measured the binding affinity between the cytoplasmic fragments of GBR1b and GBR2. We found that the addition of a C-terminal extension to the core coiled-coil sequence of each subunit did not result in more favorable enthalpic contributions, suggesting that the flanking regions have flexible conformations. Consistent with this observation, the C-termini of both GBR1bcc1 and GBR2cc1 were disordered in the crystal structure of the core coiled-coil fragment.

Previous studies have demonstrated that interaction of the coiled-coil helices of GBR1 and GBR2 is involved in shielding the retention signal in GBR1 and releasing the assembled $GABA_B$ heterodimer from the ER (9–11). First, simultaneous mutations of four hydrophobic residues in the middle of the coiled-coil domain of either subunit result in ER retention of GBR1 (9). Second, a fragment consisting of the GBR2 coiled-coil sequence is sufficient to mask the retention signal of GBR1, and the GBR2 sequence complementary to the RSRR sequence in GBR1 is not necessary for the shielding effect (11).

To identify further the specific residues that control heterodimer formation and, in turn, GBR1 surface expression, we individually mutated each residue located at the coiled-coil interface and measured its effects on GBR1b trafficking. We found that single mutations of hydrophobic residues at the center of the coiled-coil structure were sufficient to impair the cell surface expression of GBR1b. Our mutational studies confirmed that the coiled-coil interaction between $GABA_B$ subunits is responsible for

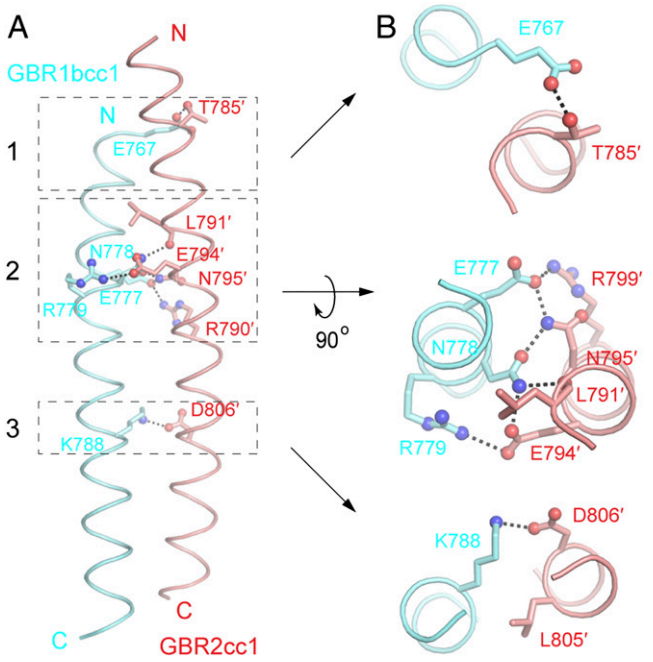

Fig. 4. Specific hydrogen bonds at the GBR1bcc1/GBR2cc1 heterodimer interface. (*A*) Ribbon representation of the GBR1bcc1/GBR2cc1 heterodimer. GBR1bcc1 and GBR2cc1 are shown in cyan and red, respectively. The locations of hydrogen bonds are highlighted in boxes. (*B*) Top view of the specific hydrogen bonds formed at the coiled-coil interface.

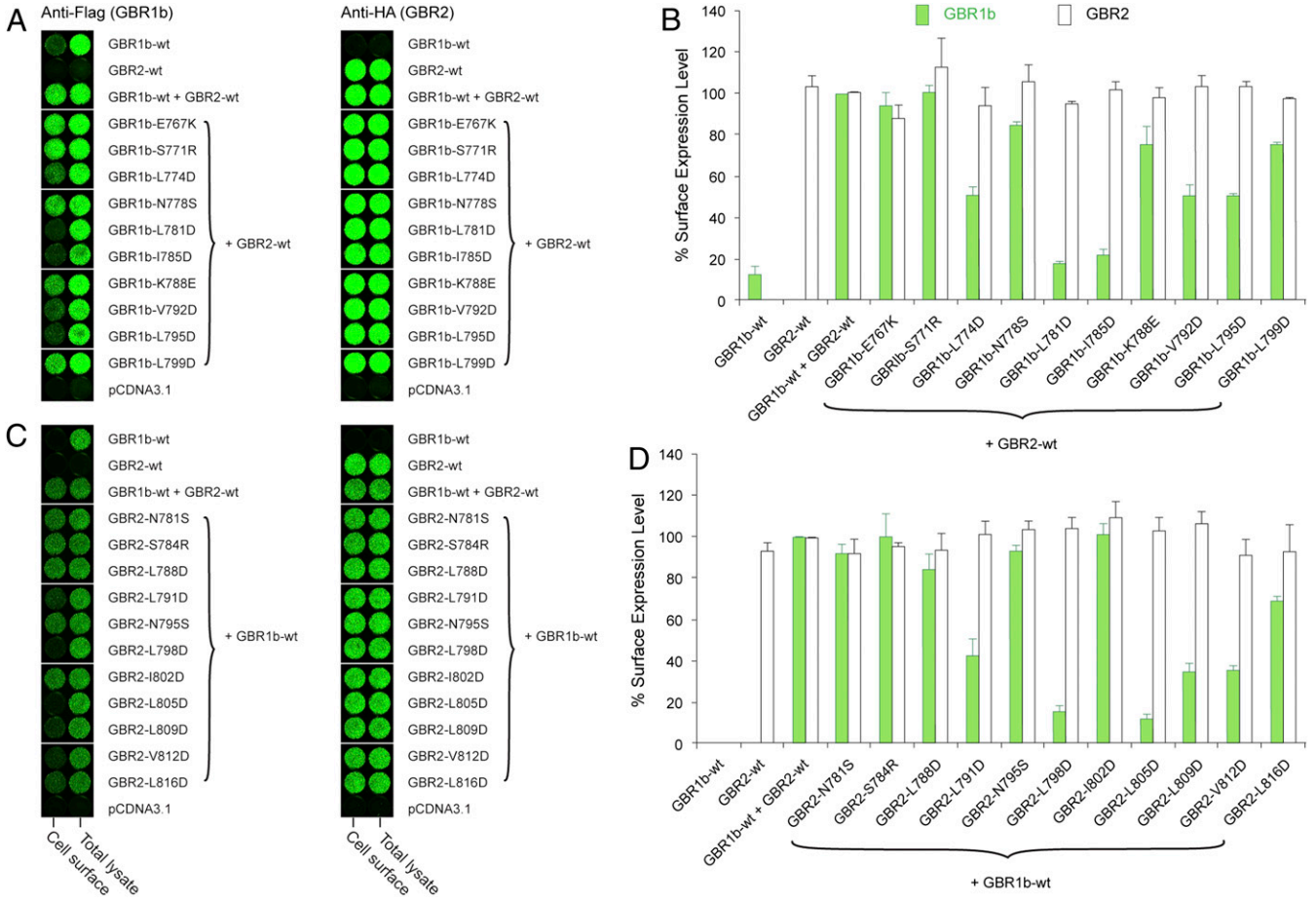

Fig. 5. Effects of coiled-coil mutations on the cell surface expression of $GABA_B$ receptor subunits. In-cell Western analysis was carried out for GBR1b mutants coexpressed with GBR2-wt (*A* and *B*) and GBR2 mutants coexpressed with GBR1b-wt (*C* and *D*). Individual $GABA_B$ receptor subunits GBR1b-wt and GBR2-wt, heterodimeric receptor GBR1b-wt + GBR2-wt, and empty vector pcDNA3.1 were included as controls. GBR1b and GBR2 were detected by anti-Flag and anti-HA antibodies, respectively. The percent surface expression levels of each $GABA_B$ subunit are summarized in a bar diagram in *B* and *D*. Data points represent average ± SEM of triplicate measurements.

masking the adjacent ER retention signal in GBR1. Because the retention signal is not part of the core coiled-coil structure, this finding supports the hypothesis that assembly of the $GABA_B$ coiled-coil heterodimer prevents ER chaperones from accessing the retention signal through steric hindrance.

Materials and Methods

Protein Expression and Purification. Genes encoding GBR1bcc and GBR2cc were amplified by PCR and inserted into the pSMT3 vector (32) for expression as small ubiquitin-like modifier (SUMO)-fusion proteins in bacteria. A His-tag was engineered at the N terminus of each construct to facilitate affinity purification. Several different pairs of coiled-coils were created, which contained different N- and C-terminal truncations of the cytoplasmic regions of GBR1b and GBR2 subunits. Specifically, GBR1bcc1 and GBR2cc1 contain residues 762–802 of GBR1b and residues 779–819 of GBR2, respectively; GBR1bcc2 and GBR2cc2 contain residues 762–810 of GBR1b and residues 779–827 of GBR2, respectively.

For each construct, the SUMO-fusion protein was expressed using BL21 (DE3) RIL cells, which contained extra copies of Arg (R), Ile (I) and Leu (L) tRNA genes. Protein production was induced at 37 °C with the addition of 1 mM isopropyl β-D-1-thiogalactopyranoside. The cells were harvested by centrifugation and lysed by sonication. The fusion protein was first purified using TALON Co^{2+}-based affinity chromatography (Clontech) and then digested with ubiquitin-like protein-specific protease (32) to remove the SUMO protein. Individual GBR1bcc and GBR2cc subunits were isolated by Superdex-75 gel filtration chromatography (GE Healthcare). They were then combined to form a coiled-coil heterodimer. The heterodimeric complex was purified by MonoQ anion exchange chromatography (GE Healthcare) followed by Superdex-75 gel filtration chromatography to separate the complex from unbound subunits.

SeMet-substituted SUMO-GBR1bcc1 and SUMO-GBR2cc1 fusion proteins were expressed in minimal media supplemented with all amino acids except for Met. Expression was induced at mid-log phase in the presence of 120 μg/mL SeMet. Purification of SeMet analogs followed the same procedure as the native proteins.

Crystallization and Structure Determination. The GBR1bcc1/GBR2cc1 heterodimer was crystallized at 20 °C in 3.0 M $(NH_4)_2SO_4$ and 0.1 M Bicine (pH 9.0). These crystals diffracted to a resolution of 1.62 Å at National Synchrotron Light Source beamline X4A. They belong to the space group $C222_1$ (a = 46.3 Å, b = 54.2 Å, c = 54.9 Å) and have one heterodimer per asymmetrical unit. SeMet crystals grew under the same conditions as the native crystals and diffracted to a resolution of 1.77 Å.

The structure of the GBR1bcc1/GBR2cc1 heterodimer was solved by the MAD method (20). Phases were evaluated using a three-wavelength dataset collected from a single SeMet crystal. The positions of the Se sites at M800 and M804 of GBR2cc1 were determined using the program HKL2MAP (33). Phase refinement and density modification were carried out in SHARP (34). The resulting electron density maps were readily interpretable and allowed us to build an initial model in O that contained all but six of the terminal residues in GBR1bcc1 and two of the terminal residues in GBR2cc1. These residues appeared to be disordered and were not visible even in the final maps. The structure was refined against the native dataset at 1.62 Å. We used Crystallography & NMR System software (35) for initial refinement and Refmac (36) in the last stages. The final model contained residues 767–801 of GBR1bcc1, residues 779–817 of GBR2cc1, and 75 water molecules. Ramachandran analysis (37) places 98.6% of all residues in favored regions

and 100% in allowed regions. The coiled-coil parameters, as defined by Crick (23), were calculated for the GBR1bcc1/GBR2cc1 complex structure using TWISTER (38).

ITC. The titration calorimetry experiments were carried out on an ITC-200 calorimeter (MicroCal) at 4 °C. Before the experiments, each protein was purified by gel filtration chromatography and dialyzed extensively against a buffer containing 20 mM Tris (pH 8.0) and 150 mM NaCl. The protein concentration of GBR2cc2 was measured from its UV absorbance at 280 nm, and its extinction coefficient was calculated based on the number of Tyr residues present in its sequence. The concentrations of GBR1bcc1, GBR1bcc2, and GBR2cc1 were determined by comparing their band densities on native and SDS gels with that of GBR2cc2. Gels were stained with Coomassie blue and quantified with a densitometer.

To determine the thermodynamics of the binding between GBR1bcc1 and GBR2cc1, GBR1bcc1 protein was placed in the sample cell at 50.1 μM, and GBR2cc1 was added to GBR1bcc1 from a 1.002 mM stock in the syringe in 1.0-μL injections. The titration was completed over the course of 25 injections. Similarly, GBR1bcc2 was placed in the sample cell at 10.38 μM and titrated with 1.0-μL injections of 182.82 μM GBR2cc2. For each titration, the heat effects of buffer dilution were measured in a control experiment, where the GBR2cc1 or GBR2cc2 protein was titrated into the buffer following the same injection schedule as the sample titration.

Data analysis was performed using MicroCal origin 5.0 software. After subtracting the control heat data, the data for the sample titration were fit to a single binding-site model.

In-Cell Western Assay. Full-length human GBR1b and GBR2 were individually cloned into a pcDNA3.1(+) vector (Invitrogen) for expression in mammalian cells. A Flag tag was inserted after the signal peptide of GBR1b, and an HA tag was placed after the signal peptide of GBR2. Mutants of GBR1b and GBR2 were constructed using the QuikChange mutagenesis system (Stratagene).

The in-cell Western blot assay involved seeding cells in 12-well cell culture plates, fixing cells after transfection, and labeling cells with epitope-specific primary antibodies followed by IR-conjugated secondary antibodies. The cells were then directly imaged in the plates. HEK 293 T/17 cells (American Type Culture Collection) were cotransfected by Lipofectamine 2000 (Invitrogen) with the GBR1b and GBR2 plasmids, and incubated at 37 °C for 24 h. The transfected cells were fixed with 4% (vol/vol) formaldehyde. Cells permeabilized with 0.5% Triton X-100 were used to determine the total expression levels of GBR1b and GBR2 in transfected cells. Untreated cells were used to determine the cell surface expression level of each subunit.

The cells were blocked with 5% (wt/vol) milk, and then incubated with mouse anti-Flag M1 antibody (Sigma) as the primary antibody to measure GBR1b expression. Similarly, mouse anti-HA antibody HA.11 clone 16B12 (Covance) was used to detect GBR2. Donkey anti-mouse IRDye 800-labeled antibody (LiCor) was used as the secondary antibody in both cases. Fluorescent signals from the cells were measured with an Odyssey Infrared Imager (LiCor). For each mutant $GABA_B$ subunit, the protein level on the cell surface was normalized against the total protein level in the cell lysate and expressed as the percent surface expression level of wild-type receptor. The results of three independent experiments were used for statistical analysis.

ACKNOWLEDGMENTS. We thank W. A. Hendrickson and R. Kass for guidance and support, L. Shapiro for advice, V. Frasca for ITC measurements, J. Schwanof (National Synchrotron Light Source) for help with data collection, and L. Mosyak for reading the manuscript. This work was supported by American Heart Association Grant SDG0835183N and National Institutes of Health Grant R01GM088454 (both to Q.R.F.). Q.R.F. is an Irma Hirschl Career Scientist, Pew Scholar, McKnight Scholar, and Schaefer Scholar.

1. Bettler B, Kaupmann K, Mosbacher J, Gassmann M (2004) Molecular structure and physiological functions of GABA(B) receptors. *Physiol Rev* 84(3):835–867.
2. Bowery NG, et al. (2002) International Union of Pharmacology. XXXIII. Mammalian gamma-aminobutyric acid(B) receptors: Structure and function. *Pharmacol Rev* 54(2): 247–264.
3. Jones KA, et al. (1998) GABA(B) receptors function as a heteromeric assembly of the subunits GABA(B)R1 and GABA(B)R2. *Nature* 396(6712):674–679.
4. Kaupmann K, et al. (1998) GABA(B)-receptor subtypes assemble into functional heteromeric complexes. *Nature* 396(6712):683–687.
5. Kuner R, et al. (1999) Role of heteromer formation in GABAB receptor function. *Science* 283(5398):74–77.
6. Ng GY, et al. (1999) Identification of a GABAB receptor subunit, gb2, required for functional GABAB receptor activity. *J Biol Chem* 274(12):7607–7610.
7. White JH, et al. (1998) Heterodimerization is required for the formation of a functional GABA(B) receptor. *Nature* 396(6712):679–682.
8. Kammerer RA, et al. (1999) Heterodimerization of a functional GABAB receptor is mediated by parallel coiled-coil alpha-helices. *Biochemistry* 38(40):13263–13269.
9. Margeta-Mitrovic M, Jan YN, Jan LY (2000) A trafficking checkpoint controls GABA(B) receptor heterodimerization. *Neuron* 27(1):97–106.
10. Calver AR, et al. (2001) The C-terminal domains of the GABA(b) receptor subunits mediate intracellular trafficking but are not required for receptor signaling. *J Neurosci* 21(4):1203–1210.
11. Pagano A, et al. (2001) C-terminal interaction is essential for surface trafficking but not for heteromeric assembly of GABA(b) receptors. *J Neurosci* 21(4):1189–1202.
12. Couve A, et al. (1998) Intracellular retention of recombinant GABAB receptors. *J Biol Chem* 273(41):26361–26367.
13. Brock C, Boudier L, Maurel D, Blahos J, Pin JP (2005) Assembly-dependent surface targeting of the heterodimeric GABAB Receptor is controlled by COPI but not 14-3-3. *Mol Biol Cell* 16(12):5572–5578.
14. Couve A, et al. (2001) Association of GABA(B) receptors and members of the 14-3-3 family of signaling proteins. *Mol Cell Neurosci* 17(2):317–328.
15. Kantamneni S, et al. (2007) GISP: A novel brain-specific protein that promotes surface expression and function of GABA(B) receptors. *J Neurochem* 100(4):1003–1017.
16. Restituito S, et al. (2005) Multiple motifs regulate the trafficking of GABA(B) receptors at distinct checkpoints within the secretory pathway. *Mol Cell Neurosci* 28(4): 747–756.
17. Kaupmann K, et al. (1997) Expression cloning of GABA(B) receptors uncovers similarity to metabotropic glutamate receptors. *Nature* 386(6622):239–246.
18. Lupas A, Van Dyke M, Stock J (1991) Predicting coiled coils from protein sequences. *Science* 252(5009):1162–1164.
19. McDonnell AV, Jiang T, Keating AE, Berger B (2006) Paircoil2: Improved prediction of coiled coils from sequence. *Bioinformatics* 22(3):356–358.
20. Hendrickson WA (1991) Determination of macromolecular structures from anomalous diffraction of synchrotron radiation. *Science* 254(5028):51–58.
21. O'Shea EK, Klemm JD, Kim PS, Alber T (1991) X-ray structure of the GCN4 leucine zipper, a two-stranded, parallel coiled coil. *Science* 254(5031):539–544.
22. Lupas AN, Gruber M (2005) The structure of alpha-helical coiled coils. *Adv Protein Chem* 70:37–78.
23. Crick FHC (1953) The packing of α-helices: Simple coiled-coils. *Acta Crystallogr* 6(8-9): 689–697.
24. Harbury PB, Zhang T, Kim PS, Alber T (1993) A switch between two-, three-, and four-stranded coiled coils in GCN4 leucine zipper mutants. *Science* 262(5138):1401–1407.
25. Grigoryan G, Keating AE (2008) Structural specificity in coiled-coil interactions. *Curr Opin Struct Biol* 18(4):477–483.
26. Lumb KJ, Kim PS (1995) A buried polar interaction imparts structural uniqueness in a designed heterodimeric coiled coil. *Biochemistry* 34(27):8642–8648.
27. Mason JM, Arndt KM (2004) Coiled coil domains: Stability, specificity, and biological implications. *ChemBioChem* 5(2):170–176.
28. O'Shea EK, Lumb KJ, Kim PS (1993) Peptide 'Velcro': Design of a heterodimeric coiled coil. *Curr Biol* 3(10):658–667.
29. Fairfax BP, et al. (2004) Phosphorylation and chronic agonist treatment atypically modulate GABAB receptor cell surface stability. *J Biol Chem* 279(13):12565–12573.
30. Guetg N, et al. (2010) NMDA receptor-dependent GABAB receptor internalization via CaMKII phosphorylation of serine 867 in GABAB1. *Proc Natl Acad Sci USA* 107(31): 13924–13929.
31. Terunuma M, et al. (2010) Prolonged activation of NMDA receptors promotes dephosphorylation and alters postendocytic sorting of GABAB receptors. *Proc Natl Acad Sci USA* 107(31):13918–13923.
32. Mossessova E, Lima CD (2000) Ulp1-SUMO crystal structure and genetic analysis reveal conserved interactions and a regulatory element essential for cell growth in yeast. *Mol Cell* 5(5):865–876.
33. Pape T, Schneider TR (2004) HKL2MAP: A graphical user interface for phasing with SHELX programs. *J Appl Cryst* 37:843–844.
34. De la Fortelle E, Bricogne G (1997) Maximum-likelihood heavy-atom parameter refinement for multiple isomorphous replacement and multiwavelength anomalous diffraction methods. *Methods in Enzymology*, eds Carter CW, Sweet RM (Academic, San Diego), Vol 276, pp 472–494.
35. Brünger AT, et al. (1998) Crystallography & NMR system: A new software suite for macromolecular structure determination. *Acta Crystallogr D Biol Crystallogr* 54(Pt 5): 905–921.
36. Winn MD, Isupov MN, Murshudov GN (2001) Use of TLS parameters to model anisotropic displacements in macromolecular refinement. *Acta Crystallogr D Biol Crystallogr* 57(Pt 1):122–133.
37. Chen VB, et al. (2010) MolProbity: All-atom structure validation for macromolecular crystallography. *Acta Crystallogr D Biol Crystallogr* 66(Pt 1):12–21.
38. Strelkov SV, Burkhard P (2002) Analysis of alpha-helical coiled coils with the program TWISTER reveals a structural mechanism for stutter compensation. *J Struct Biol* 137(1-2): 54–64.